Since January 2020 Elsevier has created a COVID-19 resource centre with free information in English and Mandarin on the novel coronavirus COVID-19. The COVID-19 resource centre is hosted on Elsevier Connect, the company's public news and information website.

Journal of Virological Methods 236 (2016) 54–61

Contents lists available at ScienceDirect

Journal of Virological Methods

journal homepage: www.elsevier.com/locate/jviromet

Standard and AEGIS nicking molecular beacons detect amplicons from the Middle East respiratory syndrome coronavirus

Ozlem Yaren[a], Lyudmyla G. Glushakova[b], Kevin M. Bradley[a], Shuichi Hoshika[a], Steven A. Benner[a,b,*]

[a] Foundation for Applied Molecular Evolution (FfAME), 13709 Progress Boulevard, Box 7, Alachua, FL 32615 USA
[b] Firebird Biomolecular Sciences LLC, 13709 Progress Boulevard, Box 17, Alachua, FL 32615, USA

Article history:
Received 11 January 2016
Received in revised form 17 June 2016
Accepted 12 July 2016
Available online 12 July 2016

Keywords:
RT-PCR
MERS-CoV
Nicking molecular beacon
Synthetic biology nucleotides

A B S T R A C T

This paper combines two advances to detect MERS-CoV, the causative agent of Middle East Respiratory Syndrome, that have emerged over the past few years from the new field of "synthetic biology". Both are based on an older concept, where molecular beacons are used as the downstream detection of viral RNA in biological mixtures followed by reverse transcription PCR amplification. The first advance exploits the artificially expanded genetic information systems (AEGIS). AEGIS adds nucleotides to the four found in standard DNA and RNA (xNA); AEGIS nucleotides pair orthogonally to the A:T and G:C pairs. Placing AEGIS components in the stems of molecular beacons is shown to lower noise by preventing unwanted stem invasion by adventitious natural xNA. This should improve the signal-to-noise ratio of molecular beacons operating in complex biological mixtures. The second advance introduces a nicking enzyme that allows a single target molecule to activate more than one beacon, allowing "signal amplification". Combining these technologies in primers with components of a self-avoiding molecular recognition system (SAMRS), we detect 50 copies of MERS-CoV RNA in a multiplexed respiratory virus panel by generating fluorescence signal visible to human eye and/or camera.

1. Introduction

1.1. MERS-CoV detection

The coronavirus that causes Middle East respiratory syndrome (MERS-CoV) is highly contagious, causing respiratory infection with high morbidity and mortality (Cheng et al., 2007; Chan et al., 2013). It first appeared in Middle East where recent reports suggest that camels are its most likely reservoir (Zaki et al., 2012; Chan et al., 2015). The most noted cases outside of that region have been in Korea, but several registered cases have appeared in the United States by "virus tourism", including in Orlando, Florida (http://www.who.int/csr/don/archive/disease/coronavirus_infections/en/).

Outside the Middle East, MERS-CoV must be diagnosed by physicians who have very little experience with its symptoms. This creates a need for a rapid molecular test for the virus, to support the early diagnosis that is needed to arrange for quarantines, manage patient care, and help public health officials track disease outbreaks.

Several molecular tests for MERS-CoV detection have been created since the 2012 American outbreak (Corman et al., 2012a,b; Lu et al., 2014). These generally use real-time RT-PCR amplification. For positive diagnosis of a MERS-CoV infection, amplification and detection of two different genomic targets is required, or sequencing that confirms a single target amplicon (http://www.who.int/csr/disease/coronavirus_infections/case_definition/en/). Culturing MERS-CoV from respiratory tract, blood, urine, or stool samples remains an option, although virus culturing is cumbersome, hazardous, and requires experienced staff to interpret cytopathic effects in host cells. Serological assays for detection of specific neutralizing anti-MERS-CoV antibodies are not ideal for early diagnosis and containment of the spread of the outbreaks. Therefore, RT-PCR based diagnostics still remains to be the most common detection method (Leland and Ginocchio, 2007; Chan et al., 2015).

Because of its instrument and power requirements, PCR cannot be used everywhere, including "low resource" environments. Therefore, tests that use isothermal amplification have been developed. These include reverse transcriptase loop-mediated isothermal amplification (LAMP) (Shirato et al., 2014) and reverse transcription recombinase polymerase amplification assays (RPA) (Abd El Wahed et al., 2013; Sharma et al., 2014). These require short incubation times, and are highly sensitive and specific, making them useful where no PCR equipment is available or operable.

* Corresponding author.
E-mail address: manuscripts@ffame.org (S.A. Benner).

http://dx.doi.org/10.1016/j.jviromet.2016.07.008
0166-0934/

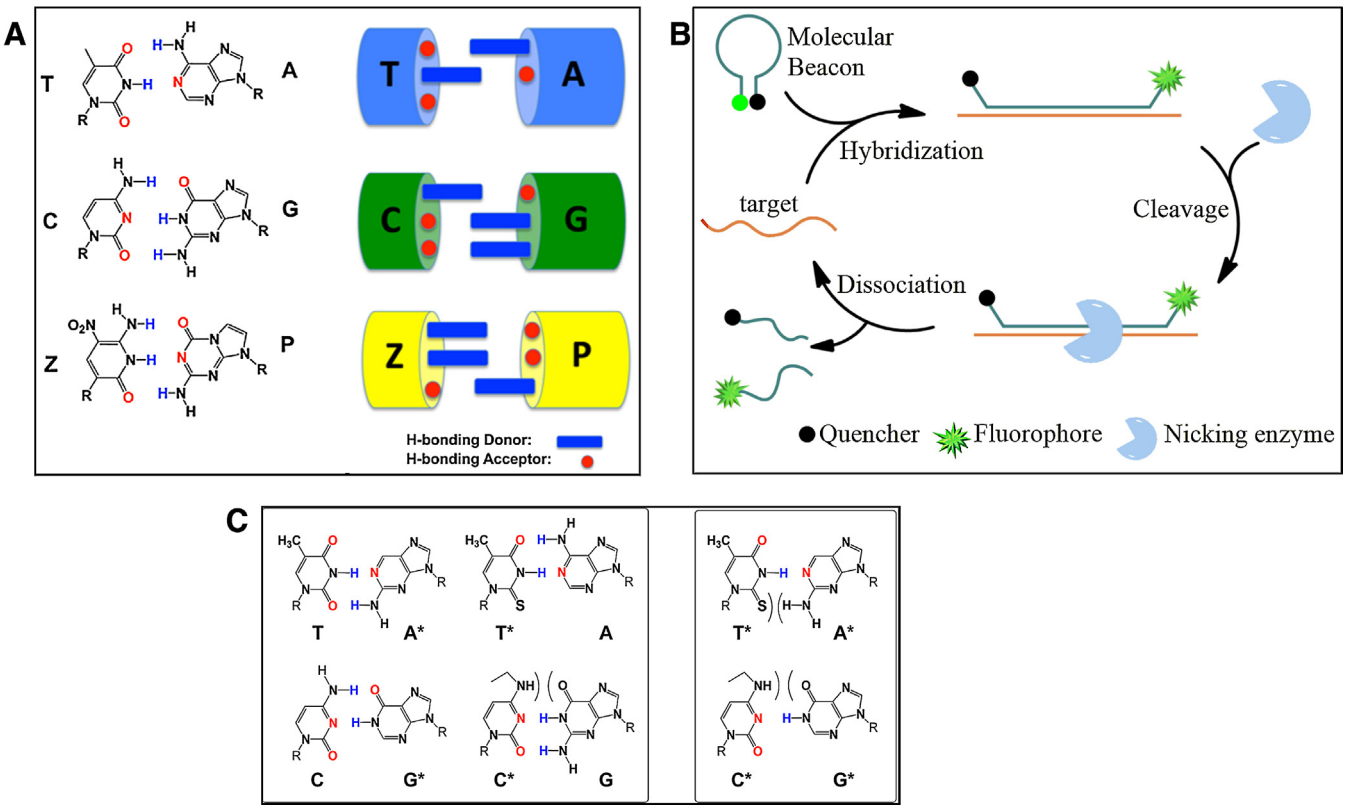

Fig. 1. (A) Components of AEGIS that, by rearranging hydrogen-bonding patterns on the nucleobases, adds six nucleotides to the four standard nucleotides. The Z:P pair was used in this assay. (B) Target DNA amplicon and complementary molecular beacon loop contains the recognition sequence of a nicking enzyme (Nt.BsmAI). When the target strand hybridizes to loop of the beacon, a full nicking enzyme recognition site forms where only MB is cut. After nicking enzyme cuts the beacon, hybrid strand becomes unstable and cleaved beacon dissociates from the target. Freed target strand can then be substrate for another molecular beacon to initiate the second cycle of cleavage thereby allowing exponential signal amplification. (C) Schematic showing that by strategic removal of hydrogen bonding groups, a SAMRS can be obtained to allow multiplexing.

Low resource environments also need inexpensive ways to detect the amplicons (Niemz et al., 2011; Boonham et al., 2014). Detection with intercalating dyes like SYBR green (Lu et al., 2014), measurements of turbidity generated by precipitating $Mg_2P_2O_7$ during amplification (Fukuda et al., 2007; Tanner et al., 2012), or luciferase-mediated bioluminescence generated from the inorganic pyrophosphate (Gandelman et al., 2010) are cheap enough, but can be deceived by off-target amplicons. Thus, melting profiles are often needed to discriminate primer artifacts from amplicon, creating extra steps, extra complexity, and extra cost.

Therefore, molecular hybridization-based methods have been favored for amplicon identification. These have sequence-specificity, reducing the likelihood of false positives. In various architectures, oligonucleotide probes may be cleaved during the amplification reaction (e.g. TaqMan) (Schultz et al., 2011), or probes/primers that change conformation upon binding to the amplicons are exploited such as scorpion primers (Carters et al., 2008) or molecular beacons (Leone et al., 1998; Zou et al., 2013).

1.2. Molecular beacons (MB)

Molecular beacons are DNA molecules with a loop complementary to the DNA or RNA (collectively xNA) analyte and a fluorescent moiety at one end and a quencher moiety at the other. A hairpin stem brings the quencher close to the fluorophore, quenching its fluorescence. When the amplicon hybridizes to the loop, it opens the beacon, separating the fluorophore from the quencher, and increasing the overall fluorescent signal (Tyagi and Kramer, 1996; Tan et al., 2004).

Thus, the signal-to-noise ratio of beacon signaling is controlled by (a) the effectiveness of the quenching in the closed stem, (b) the extent to which the open and closed beacon are in equilibrium in the absence of analyte, (c) the possibility that non-target xNA might invade the stem and open it even in the absence of analyte, and (d) the amount of fluorescence when the analyte is bound. That ratio of fluorescence from an open/closed beacon is typically between 10 and 100 (Vet and Marras, 2005).

Two approaches have been introduced to improve this ratio. For example, to prevent invasion of the stem by non-target xNA, components of an artificially expanded genetic information system (AEGIS) have been placed in the stem (Sheng et al., 2008) (Fig. 1A). AEGIS nucleotides rearrange the hydrogen bonding pattern of standard nucleotides, creating up to eight additional nucleotides that add up to four nucleobase pairs to the two pairs (A:T and G:C) found in natural nucleotides. AEGIS oligonucleotides cannot hybridize to any natural xNA, removing (c) as a factor in generating background noise. Further, AEGIS-AEGIS pairs are more stable than classical standard nucleobase pairs, minimizing background arising from (b) (Yang et al., 2006).

The consequence of a more tightly bound stem is, however, that a longer loop is required for hybridization to pull the stem apart. This problem can be mitigated by introducing a site in the loop that, when hybridized to the analyte, becomes a substrate for a nicking enzyme that cuts the loop (Fig. 1B). In the absence of cut loop, the stem is much too short to hold the fluorophore and the quencher together, so they separate as independent molecules, generating the maximum fluorescence possible.

Table 1
Hybrid SAMRS-AEGIS primers and MERS-CoV amplicons for respiratory virus panel.

Virus	Sequences (5′-3′)	Targeted region
Human respiratory syncytial virus (RSV)	Forward primer: CTAPTCCPCCAPCPA-PCGGGCAAATATGGAAACATA*C*G*T*G Reverse primer: CAGPAAGPGGTPGPTPG GGAACATGGGCACCCAT*A*T*T*G	Pneumovirus matrix protein gene
Severe acute respiratory syndrome coronavirus (SARS-CoV)	Forward primer: CTAPTCCPCCAPCPAPC GAGGAGGTTGTTCTCAAG*A*A*C*G Reverse primer: CAGPAAGPGGTPGPTPG GTAAACCAGGAGACAAT*G*C*G*C	Orf1ab polyprotein gene
Influenza A (InfA)	Forward primer: CTAPTCCPCCAPCPAPCCATG-GAATGGCTAAAGACAA*G*A*C*C Reverse primer: CAGPAAGPGGTPGPTPG CAAAGCGTCTACGCT*G*C*A*G	Segment 7 matrix protein 2 (M2) and matrix protein 1 (M1) genes
Influenza B (InfB)	Forward primer: CTAPTCCPCCAPCPAPC GATGGCCATCGGATCC*T*C*A*A Reverse primer: CAGPAAGPGGTPGPTPGTAATCGGT-GCTCTTGACCAA*A*T*T*G	Segment 8 nuclear export protein (NEP) and nonstructural protein 1 (NS1)
Middle East respiratory syndrome coronavirus (MERS-CoV) 1-2	Forward primer: CTAPTCCPCCAPCPAPCCATGC-TATTGCTTTAACGCTG*A*G*G*G Reverse primer: CAGPAAGPGGTPGPTPGGTCTCA-GAAATGCACTCTGATTCAC*C*T*T*C	ORF1a
MERS-CoV 6-1	Forward primer: CTAPTCCPCCAPCPAPC CTGGCATTGTAGCAGCTGTT*T*C*A*G Reverse primer: CAGPAAGPGGTPGPTPG GAGTGGACGTACGACAGTTG*T*A*C*C	N and ORF8b
Amplicon MERS-CoV 1-2 (145 bp)	CATGCTATTGCTTTAACGCTGAGGGTGATGCATCTTGGTCTTCT ACTATGATCTTCTCTCTTCACCCCGTCGAGTGT-GACGAGGAGTGTT CTGAAGTAGAGGCTTCAGATTTAGAAGAAGGT-GAATCAGAGTGCA TTTCTGAGAC	
Amplicon MERS-CoV 6-1 (159 bp)	CTGGCATTGTAGCAGCTGTTTCAGCTATGATGTGGATTTCCTACTTT **GTGCAGAGTATCCGGCTGTTTATGAGAACTG-GATCATGGTGGTCATT CAATCCTGAGAC-TAATTGC**CTTTTGAACGTTCCATTTGGTGGTACAA CTGTCGTACGTCCACTC	

Note: A*, T*, G*, C*: SAMRS nucleotides (Fig. 1B) and P: AEGIS nucleotide (Fig. 1C). MB recognition site is in bold.

As a further advantage to the nickase architecture, after nicking, the analyte also dissociates from the cut loop, now free to bind a second beacon loop, anneal, and direct the nicking enzyme to cleave a second beacon. This allows a single target analyte to activate more than one beacon, providing signal amplification, often by a factor of 10 (Zheleznaya et al., 2006; Li et al., 2008; Connolly and Trau, 2010).

Here we report the combination of these strategies to improve signal-to-noise with molecular beacons. The beacons contained both AEGIS in the stem and a target-specific site recognized by a nicking endonuclease in the beacon loop. To detect MERS-CoV in a respiratory panel targeting Influenza A (InfA), Influenza B (InfB), Human respiratory syncytial virus (RSV), Severe acute respiratory syndrome coronavirus (SARS-CoV) and MERS-CoV, we included SAMRS nucleotides (Fig. 1C) in the up-front PCR's primers (Hoshika et al., 2010). SAMRS nucleotides are designed not to interact with each other. Thus, SAMRS oligonucleotides added to a multiplexed nucleic acid targeted assays cannot create primer-dimer artifacts. Combined with AEGIS technology, SAMRS gives cleaner and more robust responses in assays (Yang et al., 2013; Glushakova et al., 2015a,b). Here, the combination of three innovations allowed us to successfully detect 50 viral RNA copies of MERS-CoV in authentic samples obtained from NIAID in Frederick, MD.

2. Materials and methods

2.1. Design and synthesis of oligonucleotide primers and molecular beacons

Primers and molecular beacons were designed with StrainTargeter, an in-house software package (Tables 1 and 2). StrainTargeter analyzes multiple sequence alignments (MSAs) of virus families built from public databases (GenBank, http://www.ncbi.nlm.nih.gov/genbank; ViPR, http://www.viprbrc.org; and FluDB, http://www.fludb.org), finding regions within those viral genomes that have a level of sequence divergence that allows viral targets to be distinguished, but not so much to prevent detecting viruses that are divergently evolving. A BLAST search then follows to ensure that primer and probe sequences designed by StrainTargeter are not closely similar to sequences in both the NCBI RNA virus database and the NCBI human genome database.

Two nicking molecular beacons (standard and AEGIS) were designed to detect MERS-CoV, with 6 nucleotide long stem and 26 nucleotides long loop sequence where nicking site (Nt.BsmAI, NEB) was centralized. For the AEGIS MBs, dC: dG pair in its stem was replaced by dZ: dP pair. The corresponding standard RP-HPLC purified molecular beacon purchased from Integrated DNA Technologies (IDT, Coralville, IA). It was labeled with a fluorophore, FAM, at the 5′-end, and a quencher, Black Hole Quencher-1 (BHQ-1), at 3′-end. The AEGIS molecular beacon labeled with a fluorophore, FAM, at the 5′-end, and a quencher, DABCYL, at 3′-end, was synthesized in house on ABI 394 synthesizer and RP-HPLC purified (Table 2).

2.2. Detection limit of molecular beacons

Detection sensitivity of each molecular beacon was first determined by hybridization of a short 26mer target probe (IDT, Coralville, IA) complementary to loop of the two beacons. Beacons (500 nM) were mixed with varying concentrations of complementary probe (500 nM, 200 nM, 100 nM, 50 nM, 25 nM, 10 nM, 5 nM, 1 nM, 0.5 nM, 0.1 nM and 0.05 nM) in hybridization buffer (50 μL, CutSmart® buffer, NEB: 50 mM KOAc, 20 mM Tris-acetate, 10 mM

Table 2
Molecular Beacons and probes.

Name	Targeted region	Sequence (5′-3′)
Std MB-MERS6-1	MERS 6-1	FAM-CGTGCG **CAATTAGTCTCAˆG**GATTGAATGACCA CGCACG-BHQ1
AEGIS MB-2P5Z_MERS6-1	MERS 6-1	FAM-CPTGZG CAATTA**GTCTCAˆG**GATTGAATGACCA CPCAZG-dabcyl
Target probe	MB loop	TGGTCATTCAATCCTGAGACTAATTG
MBstemtarget-6	Stem	CGTGCG
MBstemtarget-8	Stem + partial loop	CGTGCGTG
MBstemtarget-10	Stem + partial loop	CGTGCGTGGT
MBstemtarget-12	Stem + partial loop	CGTGCGTGGTCA

Note: Nicking enzyme recognition site in bold, nicking site is marked as ˆ. MB stem sequence is underlined. P and Z: AEGIS nucleotides (Fig. 1C).

MgOAc, 100 μg/mL BSA, pH 7.9, 25 °C). Thermal profiles were recorded as follows: Mixtures were first denatured at 95 °C for 1 min. The temperature was then decreased to 85 °C and held for 0.5 min. Then, the temperature was decreased slowly from 85 °C to 25 °C (programmed to occur over 70 min), with fluorescence continuously measured using Roche Light Cycler 480. For nicking enzyme-assisted signal amplification (NESA), Nt.BsmAI (20 units, 5 U/μL) was added and samples were incubated at 37 °C for about 30 min, then at 55 °C for 90 min with continuous fluorescence monitoring. Additionally, images of fluorescence generated by the beacons induced by blue LED light (470 nm) at room temperature were recorded through an orange filter by a digital camera.

2.3. MERS-CoV RNA isolation

MERS-CoV RNA was isolated according to a standard protocol (Life Technologies). Briefly, Trizol-inactivated MERS-CoV (Jordanian isolate, GenBank accession no. KC164505.2) was obtained from Lisa Hensley and Reed Johnson of the National Institute of Allergy and Infectious Diseases (Fort Detrick, Frederick, MD, USA) at a titer of 2×10^4 pfu/mL. First, chloroform (0.2 mL) was added to the virus homogenate in Trizol (1 mL). The tube was briefly vortexed (15 s) and incubated (~3 min, at room temperature). The sample was centrifuged at 12,000*g* for 15 min at 4 °C, aqueous phase collected, and glycogen added (5 mg/mL). Viral RNA was then precipitated by adding an equal volume of isopropanol at room temperature for 10 min. The RNA was pelleted by centrifugation at 10,000*g* for 10 min at 4 °C, the supernatant was removed, and the pellet was washed twice with 75% ethanol. Finally, the pellet was dissolved in the nuclease-free water (Life Technologies), aliquoted, and stored at −80 °C.

2.4. Reverse transcription PCR

Mono- (MERS-CoV specific primers only) or multiplexed one-step RT-PCR reactions (combination of MERS-CoV and RSV, SARS-CoV, InfA, InfB primers, (Table 1) including MERS-CoV RNA (100 copies) were carried out by SuperScript One-Step RT-PCR kit with Platinum Taq (Life Technologies, Carlsbad, CA). Reactions took place in 1 x reaction mix with additional $MgSO_4$ (1.5 mM, final volume, 20 μL). The reaction mixture contained 0.3 μM of each sets of forward and reverse hybrid SAMRS-AEGIS target-specific primers, and 2.5 U of RT/Platinum Taq enzyme mix. RT-PCR cycling conditions were as follows: 1 cycle of the complementary DNA (cDNA) synthesis and pre-denaturation (55 °C for 30 min and 94 °C for 2 min), 35 cycles of PCR (94 °C for 15 s, 56 °C for 30 s, and 70 °C for 30 s), and final extension at 72 °C (5 min).

2.5. Forward or reverse primer extension reactions

To favor the generation of single stranded amplicons prior to molecular beacon detection, a primer extension reaction was performed using only forward or reverse primers. Molecular beacons were designed to target the amplicons generated by forward primer (sense strand) whereas amplicons generated by reverse primer (antisense strand) served as a negative control in MB detection experiments. RT-PCR product (20 μL) was directly added to the primer extension reaction. Primer extension reaction (200 μL) was carried in 1 x ThermoPol Buffer (20 mM Tris-HCl, 10 mM $(NH_4)_2SO_4$, 10 mM KCl, 2 mM $MgSO_4$, and 0.1% Triton X-100, pH 8.8) at 25 °C (NEB, Ipswich, MA) with forward or reverse hybrid AEGIS-SAMRS primer (0.2 μM), dNTPs (0.2 mM each) and Vent (exo-) DNA polymerase (1 U per reaction; NEB). Cycling conditions were as follows: 95 °C (1 min), followed by 20 cycles (94 °C for 20 s, 56 °C for 30 s, and 72 °C for 30 s) with a final incubation cycle at 72 °C for 1 min. Reaction mixtures were then quenched with 4 mM EDTA. Amplicons (5 μL) were run on 2.5% TBE-agarose gel for visualization.

2.6. Molecular beacon detection of MERS-CoV amplicons

Primer extension products were purified by using DNA clean and concentrator kit (Zymo Research, Irvine, CA) and eluted in 50 μL of nuclease–free water. Eluted samples were divided into half (25 μL) and then mixed with 500 nM MBs (Std or AEGIS) in CutSmart® hybridization buffer (50 μL, NEB). Thermal profiles were first recorded the same way as for initial MB hybridization studies. For NESA, 20 units of Nt.BsmAI (5 U/μL, NEB) was added and samples were incubated at 37 °C for about 90 min, then at 55 °C until fluorescence curve reached saturation, with continuous fluorescence measurement. Additionally, images of fluorescence generated by a molecular beacon (with and without nicking enzyme, LED at 470 nm) at room temperature and were recorded through an orange filter by a camera.

2.7. Stem invasion of molecular beacons

To show that MB stems containing dZ and dP resist stem invasion and thereby reduce background noise, MBs (500 nM) were incubated with 2-fold excess of synthetic oligonucleotides of various lengths (IDT, 6mer, 8mer, 10mer, 12mer), each having six nucleotides complementary to the stem of the MB and a remaining sequence matching the loop region (Table 2). Thermal profiles were recorded after separately incubating these with both standard and AEGIS MBs.

3. Results

3.1. Concept of nicking enzyme signal amplification

For target-specific DNA/RNA detection, we used a special family of restriction endonucleases, DNA nicking enzymes. Nicking enzymes function as restriction enzymes, except that they cut only one strand of the recognition duplex instead of both strands (Fig. 1B).

Here we exploited a segment of the MERS-CoV virus that had the recognition sequence of Nt.BsmAI nicking enzyme. The loop of the molecular beacon contains its complement with the cleaved site. Thus, when the amplicon generated by primer extension PCR

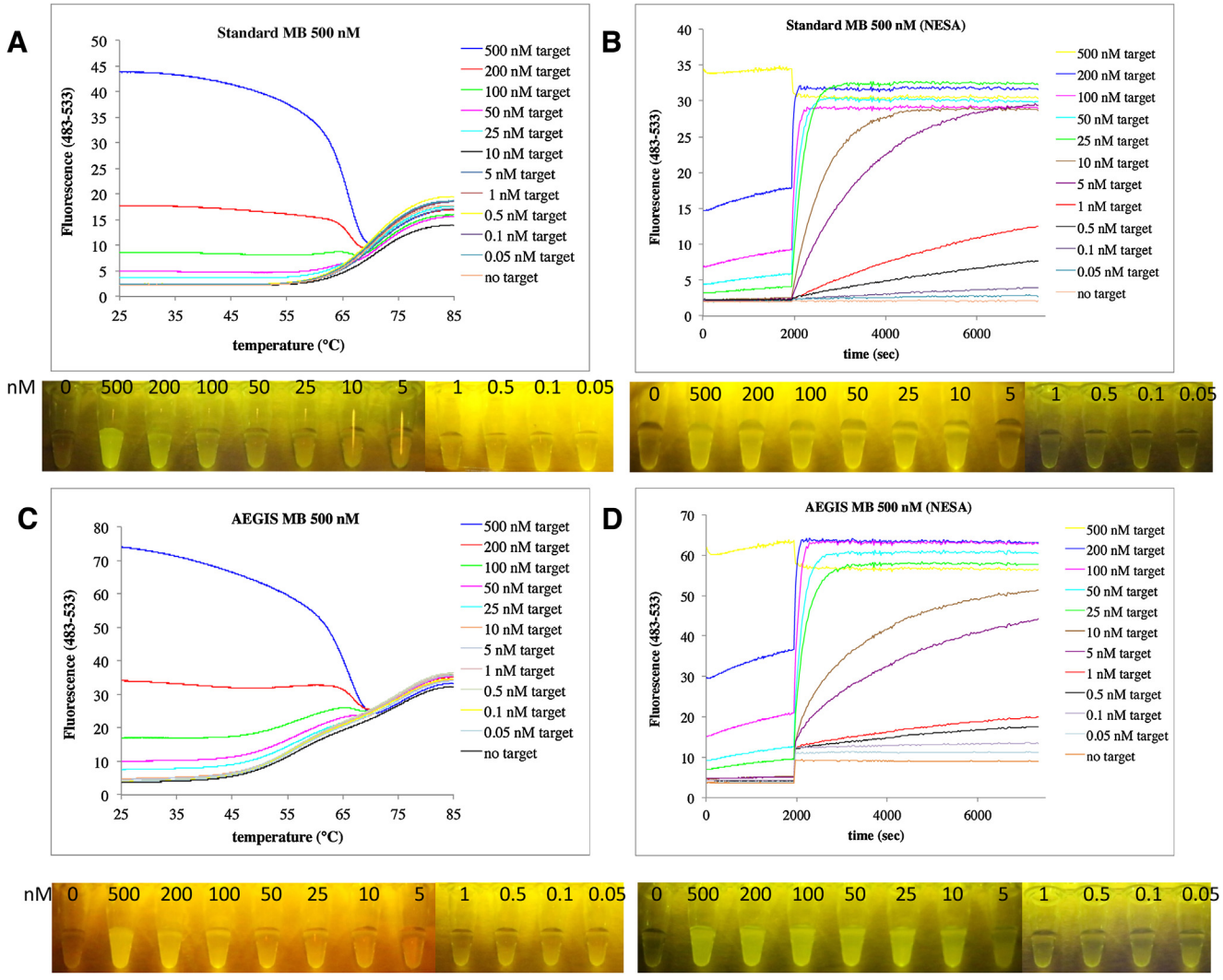

Fig. 2. (A) and (C) Thermal profiles of standard or AEGIS MBs were recorded with varying concentrations (0 to 500 nM) of short target complementary to MB loop. Time courses for NESA were recorded when nicking enzyme (Nt.BsmAI) and standard (B) or AEGIS MBs (D) were incubated with varying concentrations of short target DNA. Fluorescence intensity of each sample (before and after NESA) is recorded through an orange filter by a camera at room temperature.

hybridizes to the loop portion of the beacon, a full nicking recognition site forms where the beacon loop (not the amplicon) is cut. After the nicking reaction, the freed target strand is then available to hybridize to the loop of another molecular beacon, causing multiple cleavages, resulting in signal amplification.

3.2. Evaluation of standard and AEGIS molecular beacons

We first examined the sensitivity of the beacons in the absence of nicking enzyme. Thermal profiles were recorded by incubating standard or AEGIS MBs (500 nM) with 26mer target probe at variable concentrations ranging from 500 nM to 0.05 nM (Table 2). In the absence of the nicking enzyme, standard MB can only detect down to 200 nM (6×10^{12} copies) of target probe (Fig. 2A and Fig. 2C) while the AEGIS MB was more sensitive and was capable of detecting 100 nM target concentration (3×10^{12} copies) as have been judged by the fluorescence visible to human eye. At the lower target concentrations no significant increase in fluorescence intensity was observed.

We then repeated the assay using Nt.BsmAI. As Nt.BsmAI is optimally active at 37 °C, the mixture was first incubated at 37 °C (90 min). Then, the temperature was increased to 55 °C to help dissociation of cleaved components of molecular beacon and to favor further increase in fluorescence intensity.

Use of Nt.BsmAI improved the limit of detection (LOD) to 5 nM (10^{11} copies of target) for both MBs (Fig. 2 B and Fig. 2D). Fluorescence continued to increase up to a plateau over ~1 h, indicating beacon cleavage turnover. With complete nicking, fluorescence had increased ~14-fold. Thus, each target molecule evidently cleaved ~100 beacons, as the target:beacon ratio was 1:100 (5 nM to 500 nM). This result shows that NESA assay enables detection of otherwise undetectable amounts of target.

3.3. MERS-CoV detection with molecular beacons

To detect the MERS-CoV in real samples, we extracted primers previously used for a RT-PCR based respiratory panel targeting InfA, InfB, RSV, SARS-CoV and MERS-CoV (Glushakova et al., 2015b). These SAMRS-AEGIS forward and reverse primer pairs were tested by single-plexed assays (MERS 6-1), 2-plexed (MERS 6-1 and MERS 1-2), and 6-plexed assays (MERS-CoV 6-1, MERS-CoV 1-2, RSV, SARS-CoV, InfA and InfB) in one-step RT-PCR with 100 copies of full genomic MERS-CoV RNA followed by forward or reverse primer extension to generate single sense and antisense strands, respectively (Table 1). Each extension reaction produced the amplicon

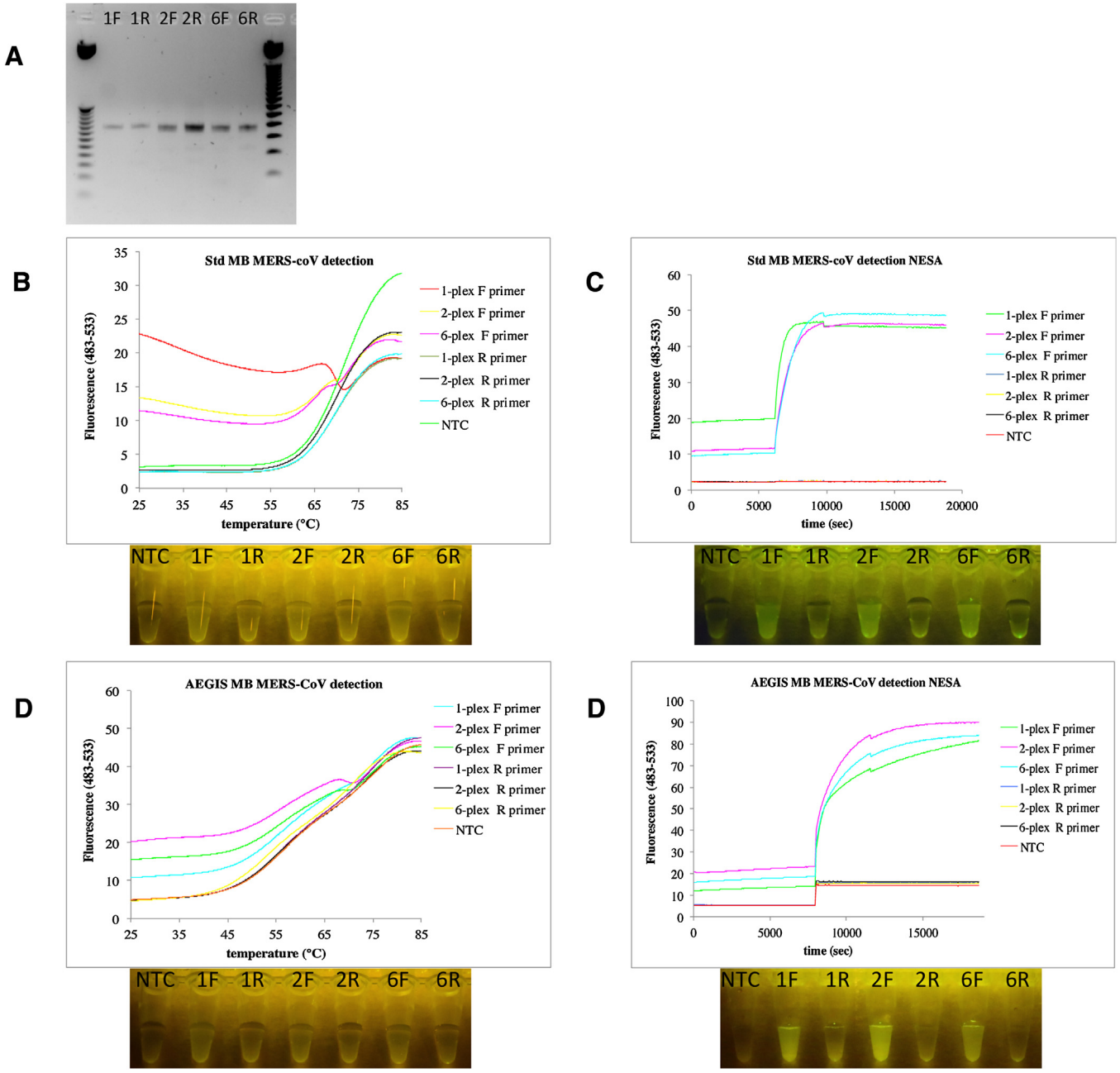

Fig. 3. (A) The sizes of single-plexed or multiplexed RT-PCR generated amplicons were confirmed by ethidium bromide staining followed by 2.5% TBE-agarose gel electrophoresis. (B) and (D) Thermal profiles of standard and AEGIS MBs were recorded with amplicons from forward or reverse primer extension reactions, respectively. (C) and (E) Time courses for NESA were recorded when nicking enzyme Nt.BsmAI and amplicons were incubated with standard or AEGIS MBs, respectively. Fluorescence intensity of each sample (before and after NESA) was recorded through an orange filter by a camera. NTC is MB only in hybridization buffer.

of the expected size, which was confirmed by agarose gel electrophoresis followed by ethidium bromide staining (Fig. 3A).

The identity of each amplicon was then confirmed by the hybridization with the target specific molecular beacons followed by NESA. Since we tested standard and AEGIS molecular beacons simultaneously, each beacon detected half of the starting MERS-CoV viral load, 50 copies in each case. Molecular beacons with the nicking sites embedded in their loops targeted the amplicon strand generated from the forward primer ("sense"). The "antisense" amplicon served as a negative control. As seen in Fig. 3B and D, both beacons successfully detect "sense" amplicons in 1-plexed, 2-plexed and 6-plexed assays.

Signal amplification was more pronounced when nicking enzyme was included in the detection assay. Moreover, this assay was target-specific, because amplicons from the opposite strand failed to produce a change in fluorescence (Fig. 3C and E). It is also notable that total fluorescence intensity was higher by 1.6-fold when the MERS-CoV amplicon was used as a target rather than a synthetic RNA simulant. This showed that in addition to being complementary to the beacon loop, the amplicon from the MERS-CoV genome had an additional nucleotide complementary to the first (standard) nucleotide in the stem (Figs. 2 D and 3 E). This improved the efficiency of target hybridization, NESA-induced cleavage, and downstream dissociation of the cleaved fragments.

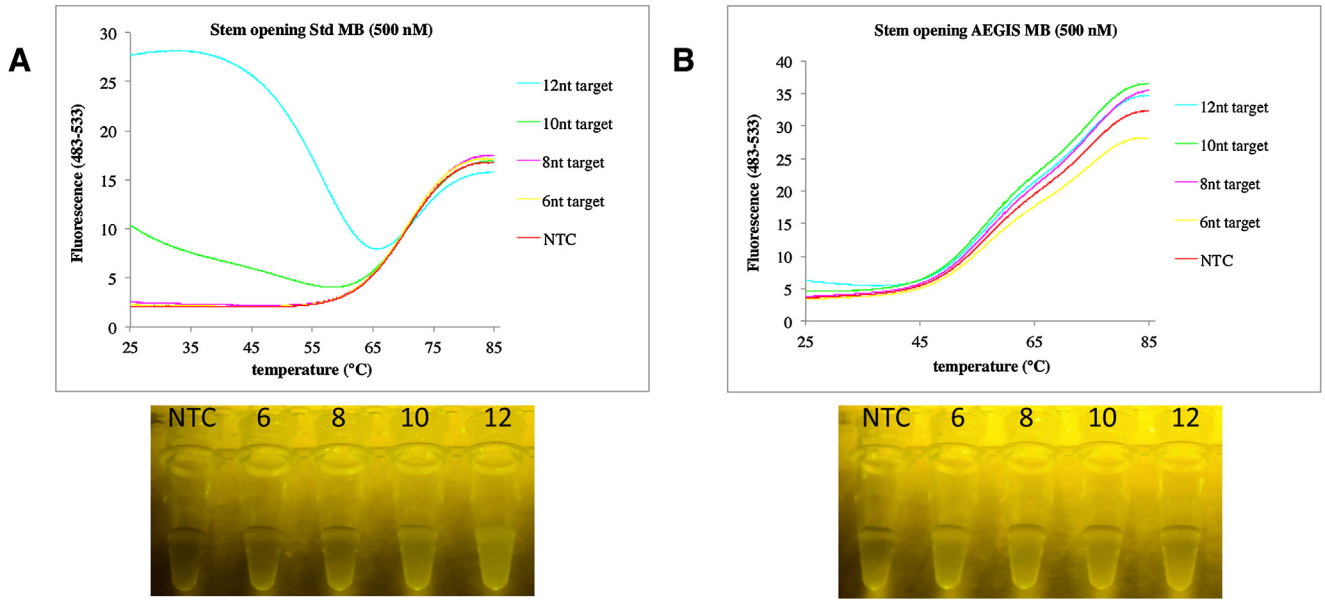

Fig. 4. Stem invasion experiments. Thermal profiles of (A) standard and (B) AEGIS MBs incubated with synthetic oligonucleotides in various lengths that had six nucleotides complementary to the stem of the MB, and a remaining sequence matched the loop region, were recorded followed by a digital camera imaging.

Most importantly, the AEGIS MB exhibited higher fluorescence signal than the standard MB. Total fluorescence intensity increased by 1.8-fold when MERS-CoV viral genome was present (Fig. 3C and E).

3.4. Stem invasion assay

To show that MB stems with dZ and dP reduce the background fluorescence by resisting the stem invasion, MBs (500 nM) were incubated with 2-fold excess of synthetic oligonucleotides having various lengths (6mer, 8mer, 10mer, 12mer) that had six nucleotides complementary to the stem of the MB, and a remaining sequence matched the loop region (Table 2). Thermal profiles were recorded after separately incubating these with both standard and AEGIS MBs and camera images are also taken at room temperature for visualization. For standard MB, incubation with 2-fold excess of the 6mer failed to open the beacon, while 8mer DNA target exhibited slight increase in fluorescence. This was consistent with the design strategy that intramolecular binding constant between the stem sequences is far greater than the intermolecular interaction between one arm of the stem and short DNA targets (6mer or 8mer). On the other hand, in the presence of the 10mer and 12mer targets, stem and part of the loop of the MB hybridized to the target, disrupted the hairpin structure, and increased the background fluorescence by 24% and 62%, respectively (Fig. 4A). In contrast, AEGIS-containing MB was not opened by any of the stem targets tested except with the 12mer target where only slight increase in fluorescence is observed (Fig. 4B). These results suggest that AEGIS-modified molecular beacons are superior to standard beacons in terms of resistance to stem invasion and overall NESA efficiency.

4. Discussion

Multiplexed PCR-based assays that target the multiple possible causes of respiratory infection often fail because multiple primers, presented at high concentrations, interact with each other to divert amplification resources and form artifacts, including primer-dimers and extension products of nonspecifically paired primers, often imperfectly matched. These non-specific reactions often lead to false negatives in nucleic acid-targeted assays (Elnifro et al., 2000).

To support the high levels of multiplexing, we previously developed SAMRS for primers (Hoshika et al., 2010). Here we showed again that SAMRS-AEGIS primers improved the performance of the multiplexed RNA-targeted amplification.

In addition to SAMRS-AEGIS technologies, we explored a new signal amplification mechanism to improve the sensitivity of the molecular beacons. Molecular beacons have an advantage over traditional DNA probes by generating an “on” or “off” signal. Ideally, they do not emit fluorescence until target is hybridized to beacon to separate quencher from the fluorophore. Although their simplicity of function makes them attractive for direct detection, their intrinsic background and interaction with adventitious xNA limits their sensitivity to high nano-molar concentrations of target (Zhang et al., 2001; Drake and Tan, 2004).

Thus, their ability to detect low concentrations of DNA or RNA benefits from amplification at the detection step as well. This was obtained here using a nicking enzyme, boosting the sensitivity by 1–2 orders of magnitude, enough to allow a signal to be visible from just 10^{10}–10^{11} copies of amplicon.

The sensitivity of NESA was further improved, especially in complex assay mixtures, by adding AEGIS nucleotides to the beacon stems. This eliminated unwanted stem invasion by DNA complementary to the nucleotide sequence in the stem.

In a combination using AEGIS in a nicking molecular beacon, we were able to detect 50 copies of MERS-CoV in a real sample, and in an assay that could also detect influenza, RSV and other less exotic species that might cause the respiratory infection in an admitted patient. This allows a physician to rapidly distinguish a patient having one of these common infections from a patient that has an unusual (at least in the United States) MERS-CoV infection.

Acknowledgments

Inactivated MERS-CoV (Jordanian isolate, GenBank accession no: KC164505.2) was kindly provided by Lisa Hensley and Reed Johnson of the National Institute of Allergy and Infectious Diseases. This study was supported by the Defense Threat Reduction

Agency (DTRA, HDTRA1-13-1-0004) and National Institute of Health (R41AI116445-01, 1R41GM115130-01A1).

References

Abd El Wahed, A., Patel, P., Heidenreich, D., Hufert, F.T., Weidmann, M., 2013. Reverse transcription recombinase polymerase amplification assay for the detection of middle east respiratory syndrome coronavirus. PLoS Curr. 5, 1–11.

Boonham, N., Kreuze, J., Winter, S., van der Vlugt, R., Bergervoet, J., Tomlinson, J., Mumford, R., 2014. Methods in virus diagnostics: from ELISA to next generation sequencing. Virus Res. 186, 20–31.

Carters, R., Ferguson, J., Gaut, R., Ravetto, P., Thelwell, N., Whitcombe, D., 2008. Design and use of scorpions fluorescent signaling molecules. In: Marx, A., Seitz, O. (Eds.), Molecular Beacons: Signalling Nucleic Acid Probes, Methods, and Protocols. Humana Press, pp. 99–115.

Chan, J.F., Lau, S.K., To, K.K., Cheng, V.C., Woo, P.C., Yuen, K.Y., 2015. Middle East respiratory syndrome coronavirus: another zoonotic betacoronavirus causing SARS-like disease. Clin. Microbiol. Rev. 28, 465–522.

Chan, J.F.-W., Lau, S.K.-P., Woo, P.C.-Y., 2013. The emerging novel Middle East respiratory syndrome coronavirus: the knowns and unknowns. J. Formosan Med. Assoc. 112, 372–381.

Cheng, V.C., Woo, P.C.Y., Yuen, K.Y., 2007. Severe acute respiratory syndrome coronavirus as an agent of emerging and reemerging infection. Clin. Microbiol. Rev. 20, 660–694.

Connolly, A.R., Trau, M., 2010. Isothermal detection of DNA by beacon-assisted detection amplification. Angew. Chem. Int. Ed. 49, 2720–2723.

Corman, V.M., Eckerle, I., Bleicker, T., Zaki, A., Landt, O., Eschbach-Bludau, M., van Boheemen, S., Gopal, R., Ballhause, M., Bestebroer, T.M., Muth, D., Muller, M.A., Drexler, J.F., Zambon, M., Osterhaus, A.D., Fouchier, R.M., Drosten, C., 2012a. Detection of a novel human coronavirus by real-time reverse-transcription polymerase chain reaction. Euro Surveill 17, 20285.

Corman, V.M., Muller, M.A., Costabel, U., Timm, J., Binger, T., Meyer, B., Kreher, P., Lattwein, E., Eschbach-Bludau, M., Nitsche, A., Bleicker, T., Landt, O., Schweiger, B., Drexler, J.F., Osterhaus, A.D., Haagmans, B.L., Haagmans, B.L., Dittmer, U., Bonin, F., Wolff, T., Drosten, C., 2012b. Assays for laboratory confirmation of novel human coronavirus (hCoV-EMC) infections. LID – 20334 [pii]. Euro Surveill 17, 20334.

Drake, T.J., Tan, W., 2004. Molecular beacon DNA probes and their bioanalytical applications. Appl. Spectrosc. 58, 269A–280A.

Elnifro, E.M., Ashshi, A.M., Cooper, R.J., Klapper, P.E., 2000. Multiplex PCR: optimization and application in diagnostic virology. Clin. Microbiol. Rev. 13, 559–570.

Fukuda, S., Sasaki, Y., Kuwayama, M., Miyazaki, K., 2007. Simultaneous detection and genogroup-screening test for norovirus genogroups I and II from fecal specimens in single tube by reverse transcription- loop-mediated isothermal amplification assay. Microbiol. Immunol. 51, 547–550.

Gandelman, O.A., Church, V.L., Moore, C.A., Kiddle, G., Carne, C.A., Parmar, S., Jalal, H., Tisi, L.C., Murray, J.A.H., 2010. Novel bioluminescent quantitative detection of nucleic acid amplification in real-time. PLoS One 5, e14155.

Glushakova, L.G., Bradley, A., Bradley, K.M., Alto, B.W., Hoshika, S., Hutter, D., Sharma, N., Yang, Z., Kim, M.-J., Benner, S.A., 2015a. High-throughput multiplexed xMAP Luminex array panel for detection of twenty two medically important mosquito-borne arboviruses based on innovations in synthetic biology. J. Virological Methods 214, 60–74.

Glushakova, L.G., Sharma, N., Hoshika, S., Bradley, A.C., Bradley, K.M., Yang, Z., Benner, S.A., 2015b. Detecting respiratory viral RNA using expanded genetic alphabets and self-avoiding DNA. Anal. Biochem. 489, 62–72.

Hoshika, S., Chen, F., Leal, N.A., Benner, S.A., 2010. Artificial genetic systems: self-avoiding DNA in PCR and multiplexed PCR. Angew. Chem. Int. Ed. 49, 5554–5557.

Leland, D.S., Ginocchio, C.C., 2007. Role of cell culture for virus detection in the age of technology. Clin. Microbiol. Rev. 20, 49–78.

Leone, G., van Gemen, B., Schoen, C.D., van Schijndel, H., Kramer, F.R., 1998. Molecular beacon probes combined with amplification by NASBA enable homogeneous, real-time detection of RNA. Nucleic Acids Res. 26, 2150–2155.

Li, J.J., Chu, Y., Lee, B.Y.-H., Xie, X.S., 2008. Enzymatic signal amplification of molecular beacons for sensitive DNA detection. Nucleic Acids Res. 36, e36–e36.

Lu, X., Whitaker, B., Sakthivel, S.K.K., Sakthivel, S.K., Kamili, S., Rose, L.E., Lowe, L., Mohareb, E., Mohareb, E., Elassal, E.M., Al-sanouri, T., Haddadin, A., Erdman, D.D., 2014. Real-time reverse transcription-PCR assay panel for Middle East respiratory syndrome coronavirus. J. Clin. Microbiol. 52, 67–75.

Niemz, A., Ferguson, T.M., Boyle, D.S., 2011. Point-of-care nucleic acid testing for infectious diseases. Trends Biotechnol. 29, 240–250.

Schultz, A.C., Vega, E., Dalsgaard, A., Christensen, L.S., Norrung, B., Hoorfar, J., Vinje, J., 2011. Development and evaluation of novel one-step TaqMan realtime RT-PCR assays for the detection and direct genotyping of genogroup I and II noroviruses. J. Clin. Virol. 50, 230–234.

Sharma, N., Hoshika, S., Hutter, D., Bradley, K.M., Benner, S.A., 2014. Recombinase-based isothermal amplification of nucleic acids with self-avoiding molecular recognition systems (SAMRS). ChemBioChem 15, 2268–2274.

Sheng, P., Yang, Z., Kim, Y., Wu, Y., Tan, W., Benner, S.A., 2008. Design of a novel molecular beacon: modification of the stem with artificially genetic alphabet. Chem. Comm. 7, 5128–5130.

Shirato, K., Yano, T., Senba, S., Akachi, S., Kobayashi, T., Nishinaka, T., Notomi, T., Matsuyama, S., 2014. Detection of Middle East respiratory syndrome coronavirus using reverse transcription loop-mediated isothermal amplification (RT-LAMP). Virol. J. 11, 139–149.

Tan, W., Wang, K., Drake, T.J., 2004. Molecular beacons. Curr. Opin. Chem. Biol. 8, 547–553.

Tanner, N.A., Zhang, Y., Evans Jr., T.C., 2012. Simultaneous multiple target detection in real-time loop-mediated isothermal amplification. BioTechniques 53, 81–89.

Tyagi, S., Kramer, F.R., 1996. Molecular beacons: probes that fluoresce upon hybridization. Nat. Biotech. 14, 303–308.

Vet, J.M., Marras, S.E., 2005. Design and optimization of molecular beacon real-time polymerase chain reaction assays. In: Herdewijn, P. (Ed.), Oligonucleotide Synthesis. Humana Press, 273-290.

Yang, Z., Durante, M., Glushakova, L.G., Sharma, N., Leal, N.A., Bradley, K.M., Chen, F., Benner, S.A., 2013. Conversion strategy using an expanded genetic alphabet to assay nucleic acids. Anal. Chem. 85, 4705–4712.

Yang, Z., Hutter, D., Sheng, P., Sismour, A.M., Benner, S.A., 2006. Artificially expanded genetic information system: a new base pair with an alternative hydrogen bonding pattern. Nucleic Acids Res. 34, 6095–6101.

Zaki, A.M., van Boheemen, S., Bestebroer, T.M., Osterhaus, A.D.M.E., Fouchier, R.A.M., 2012. Isolation of a Novel Coronavirus from a Man with Pneumonia in Saudi Arabia. N. Engl. J. Med. 367, 1814–1820.

Zhang, P., Beck, T., Tan, W., 2001. Design of a molecular beacon DNA probe with two fluorophores. Angew. Chem. Int. Ed. 40, 402–405.

Zheleznaya, L.A., Kopein, D.S., Rogulin, E.A., Gubanov, S.I., Matvienko, N.I., 2006. Significant enhancement of fluorescence on hybridization of a molecular beacon to a target DNA in the presence of a site-specific DNA nickase. Anal. Biochem. 348, 123–126.

Zou, B., Ma, Y., Zhou, G., 2013. DNA detection by cascade enzymatic signal amplification. Methods Mol. Biol. 1039, 131–137.